



ARTICLE

Fabrication of Crack-Free Flattened Bamboo and Its Macro-/Micro-Morphological and Mechanical Properties

Zhichao Lou^{1,2}, Tiancheng Yuan¹, Qiuyi Wang¹, Xinwu Wu¹, Shouheng Hu¹, Xiaomeng Hao¹, Xianmiao Liu^{3,*} and Yanjun Li^{1,*}

¹College of Materials Science and Engineering, Nanjing Forestry University, Nanjing, 210037, China

²Key Laboratory of National Forestry and Grassland Administration/Beijing for Bamboo & Rattan Science and Technology, Beijing, 100102, China

³International Center for Bamboo and Rattan, Beijing, 100102, China

*Corresponding Authors: Xianmiao Liu. Email: liuxm206@163.com; Yanjun Li. Email: nfc2018@163.com

Received: 15 September 2020 Accepted: 17 October 2020

ABSTRACT

This work aimed to help the bamboo industry develop methodology for producing imperfection-free bamboo boards that can serve either decorative or structural benefit to consumers seeking to engage with the bioeconomy. Specifically, softened and slotted bamboo tubes were handled by a roller device with nails to render crack-free flattened bamboo board. Softening temperature and time were optimized herein according to findings regarding chemical composition and board mechanical properties. The optimal softening parameters for saturated steam heat treatment is proved to be 160°C for 8 min. The flattened bamboo board possesses an increased bending strength of 101.5 MPa and a decreased bending modulus of 7.7 GPa, being compared with only-softened bamboo. The corresponding changing mechanism is determined in-depth by the micro-morphological and mechanical results based on *in-situ* SEM and AFM technologies. Under the action of nails and rolling processes, the bamboo texture becomes compact with crushed and fragmented conduit walls. The resulting cell cavity then becomes stretched and compressed, taking on a morphology which allows for the mechanical penalties associated with flattening to be avoided. According to the micro-mechanical results obtained by AFM, compared with unflatten bamboo, the Young's modulus of the cell membrane in transverse direction (YT) decreases to 1.00 GPa while the corresponding Young's modulus in radial direction (YR) increases to 7.29 GPa.

KEYWORDS

Flattened bamboo board; saturated steam heat treatment; macro-mechanics; *in-situ* atomic force microscopy; young's modulus; micromorphology

1 Introduction

Over the last 30 years, the Chinese bamboo industry has been able to distinguish itself globally as a leader in the fields of bamboo processing technology and product research. So far, multiple structural and decorative engineered bamboo products, such as bamboo plywood [1], laminated bamboo strips lumber [2], wood-bamboo composite [3], sliced bamboo veneer [4], and bamboo reconstituted timber [5], have



been developed, promoting the technological progress of bamboo processing industry. However, the current practice for manufacturing bamboo-based products involves cutting bamboo tubes along the grain followed by planing, gluing, pressing, and other finishing processes. The disadvantages of this approach mainly include low raw materials utilization rate (25–45% of raw material), poor environment friendly performance (serious dust pollution and more resin consumption), and poor ability to maintain the original texture of bamboo. Each of these issues compounds and seriously restricts further development and expansion of bamboo processing industry beyond China's borders [6,7]. One method for overcoming these limitations that has been under investigation in 1980s, which is first proposed by Prof. Zhang, is to simply flatten bamboo tubes into straight board-like materials [8]. By adopting this approach, the existing cumbersome operations associated with bamboo product manufacture can be remediated via higher raw material utilization rates and a wider range of applications for the resultant products.

The first generation of flattened bamboo boards were manufactured as bamboo sheets produced via softening, flattening, drying, and shaping the raw material. Due to the small diameter and large curvature of wild bamboo, the outer surface must undergo squeezing to disrupt its mechanical interlocking while the inner surface must be stretched to allow for a more uniform board to take shape [9]. With respect to these initial processes, Zhang et al. describe a technology referred to as 'high temperature softening and flattening' which produces bamboo plywood used as truck platform floors. However, this process has been found to be prone to rendering obvious cracks on the board surface. This unavoidable outcome has been attributed to the fact that the tensile stress on the inner surface is much greater than the allowable stress in the transverse direction of bamboo [8]. As a result, the obtained products are difficult to be used as decorative materials due to the undesirable visuals imbued upon flattening [10]. Various alternative methods have been introduced to solve this problem. For example, Qian et al. optimized the softening procedure by increasing the temperature and moisture content [11]. Alternatively, Jiang et al. used chain conveying softening machine to soften bamboo at high temperature prior to flattening [12]. However, due to the unique structural features of bamboo, these approaches have been found to only consistently render high quality products for bamboo blocks with small radian. When bamboo blocks have larger radian, undesirable cracks and other visual defects return.

Taking aiming at the problems in the existing technology mentioned above, a new approach involving a saturated steam heat treatment process has been developed. Performed upon the slotted bamboo tube, this additional treatment process appears to enable manufacture of crack-free flattened bamboo [13]. By doing this, the modulus of elasticity of bamboo is reduced. Additionally, the stress release of the bamboo tube growth is realized when this approach is further integrated with other new technologies such as inner surface nicking [14,15]. A graphical depiction of the whole production process is shown in Fig. 1A. At the conclusion of these operations, crack-free flattened bamboo boards are rendered. A photograph of the final product is shown in Fig. 1B. The success of this approach is mainly due to the fact that the saturated steam heat treatment delivers higher temperatures to bamboo compared with general hydrothermal or dry heat treatment [16]. This strategy ensures that the temperature of non-crystalline cellulose inside bamboo can reach its glass transition temperature [17]. As a result, the corresponding transverse elastic modulus of the bamboo decreases, the plasticity increases, and a completely softened bamboo board is obtained. And compared with other heat treatment methods, the hot steam not only condenses on the surface of the treated bamboo tubes, thus releasing a large amount of heat, but also keeps the treated bamboo tubes with high moisture content during the heat treatment, which facilitates the rapid heat transfer inside bamboo. In this situation the manufacturer improves heating efficiency and reduces the softening time [18,19]. Recently, more and more attentions have been paid on saturated steam heat treatment which is supposed to be more economical and eco-friendlier than traditional methods. Besides, moderate saturated steam heat treatment has been proved to effectively improve the physical and mechanical properties of bamboo-based materials [20,21].

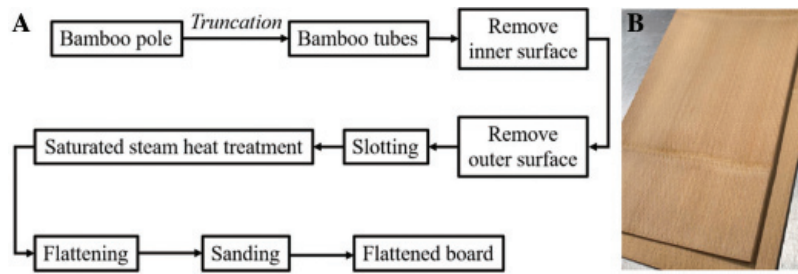


Figure 1: (A) Production process of flattened bamboo board. (B) Physical photo of obtained flattened bamboo board

There are several published works which have effectively investigated the influence of temperature, time and initial moisture content on the properties of saturated steam-treated bamboo products [16,22,23]. The main chemical components of bamboo are lignin, hemicellulose and cellulose. They have different glass transition temperature (T_g), which are 100°C , 80°C , and $130\sim 150^\circ\text{C}$, respectively [24–26]. If the softening temperature is too low to reach the glassy temperature of these biomass components, the bamboo tubes will be difficult to be flattened, and the obtained plates are easy to crack. However, excessive softening at higher temperature can easily lead to degradation of the biomass components, which is harmful to the corresponding physical and mechanical properties [27]. Meanwhile, the temperature and time of saturated steam heat treatment also relate to the actual production efficiency, energy consumption and cost. In current production process, the softening parameters are not uniform, which leads to a great difference in properties of flattened bamboo plates produced by different manufacturers and from different regions in China. As one could imagine, this variability is not conducive to standardized production and sales of flattened bamboo materials. Considering this, four-year-old bamboo tubes with removing inner and outer surface which also have undergone longitudinally slotting were evaluated as subjects for the current work. Changes to chemical composition, crystallinity, color, and mechanical properties were studied under the saturated steam heat treatment using different temperatures (140°C – 180°C) and exposure times (4–10 min). From this, optimized softening process parameters were determined for practical industrial production of flattened bamboo products. In addition, the micro-morphology and mechanical properties of the samples were also investigated to explain the mechanisms for the changes in macro-mechanics. The obtained flattened bamboo board is expected to be used in home decoration, bamboo structural materials, bamboo flooring and many other fields [28–31]. This work will serve as a foundational reference for those seeking to streamline the fledgling bamboo board industry in China in order to encourage greater assimilation of these sustainable materials into the global biomaterial economy.

2 Materials and Methods

2.1 Materials

Natural 4-year-old Moso bamboo was taken from Qingyuan City, Zhejiang Province in China. The fresh bamboo with a initial moisture content of 60–80% was cut at a joint with a height of about 1.0 m above the ground, and further cut into tubes with lengths of 60 cm. Cut bamboo tubes with an outer diameter of 100 mm and a wall thickness of ~ 10 mm were then hand-selected for further investigation.

2.2 Methods

Selected bamboo tubes were divided into 21 groups with 10 tubes in each group, among which one group that was used as a control.

2.2.1 Removal of Inner/Outer Knot and Inner Surface of Bamboo Tubes

The bamboo tube partitions were first broken, and the inner knots were removed using floating milling technology on a continuous integrated machine [32]. Briefly, the combined milling cutter is inserted into the bamboo tube and the punch then breaks through the partition. Next, the bamboo tube is supported and rotated by four rubber friction wheels with an opposite direction to the milling cutter. This apparatus is shown in Fig. 2A. Because of unavoidable asymmetrical pressurization of the cylinders in two directions, the inner wall of the bamboo tube is closer to the outer circumference of the limit ring while and the inner wall of the bamboo tube is used as the basis for milling. Then, the treated specimen are immediately clamped from both ends and rotated along a milling head as shown in Fig. 2B, in order to remove the outer knots and layers of the bamboo tubes [33]. The milling head moves from one end to another along the bamboo tube axis. Radial pressure of the milling cutter acting on the bamboo tube is adjusted on the machine, and the limit ring is close to the outer wall of the milled bamboo tube so that the milling head floats up and down with changes to the surface features of each bamboo tube. The whole procedure overcomes the challenges presented by unavoidable growth defects in some bamboo tubes. To be mentioned, no moisture content requirement is needed for the tubes before this procedure.

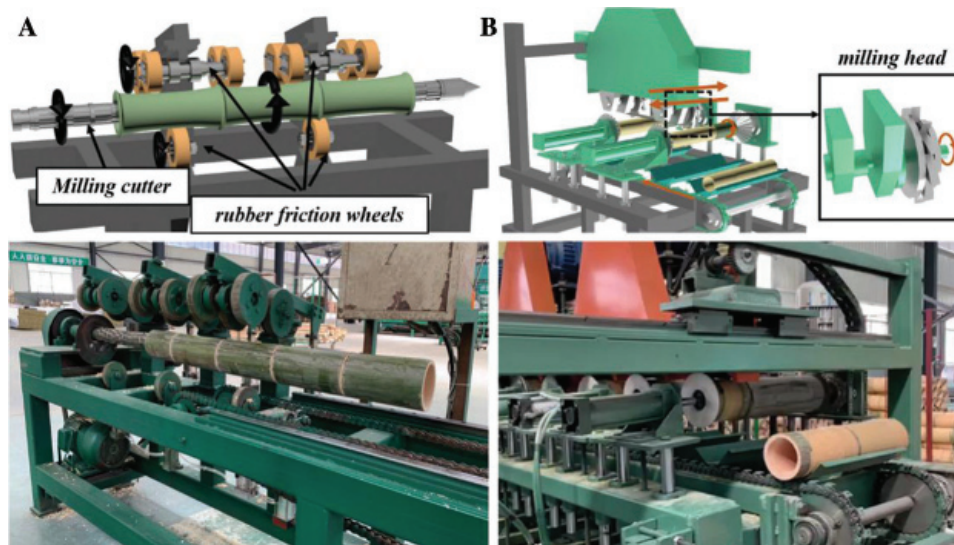


Figure 2: (A) Schematic (top) and physical picture (bottom) of the machine for removing bamboo tube's inner knots and layer. (B) Schematic (top) and physical picture (bottom) of the machine for removing the outer knots and layer

2.2.2 Saturated Steam Heat Treatment

After the removal of the inner layer and the outer layer, the bamboo tube was next longitudinally slotted by a circular saw, as shown in Fig. 3A. After flattening along the obtained groove line, the bamboo tube is transformed into a bamboo plate with a wider width.

The bamboo tubes were heated in saturated steam heat treatment equipment at different temperature (140, 150, 160, 170 and 180°C) and with different time (4, 6, 8 and 10 min). The initial moisture content of the samples was controlled as 50% before the treatment.

2.2.3 Flattening Treatment

Before the softening procedure, the bamboo tubes are firstly slotted by a rotating serrated blade following their radial directions as shown in Fig. 3A. As the density, hygroscopicity, and cellulose

contents are distributed over gradient from inner surface to bamboo flesh, and to outer surface of bamboo tubes, the slotted notch will be widened during saturated steam heat treatment, as shown in Fig. 3B. This is an important prerequisite for bamboo tube flattening. Only when the notch becomes wide enough can the softened bamboo tube enter the horizontal flattener apparatus as shown in Fig. 3C. To be mentioned, the treated samples should be put into the flattener apparatus immediately after the softening procedure, in order to ensure that the samples can be flattened under the condition of high temperature and high humidity. As shown in Fig. 3C(2), the horizontal flattener apparatus is equipped with a couple of rollers. The upper roller is smooth, which is convenient for the softened bamboo tube to enter the flattener. Differently, there are nails on the surface of the lower roller. In the process of flattening, these nails pierce into the inner surface of the bamboo tube with a depth value of 3 mm, to release the flattening stress and avoid cracks. After being cooled and shaped by rolling as shown in Fig. 3D, a flattened bamboo board with nail holes on one surface is obtained.

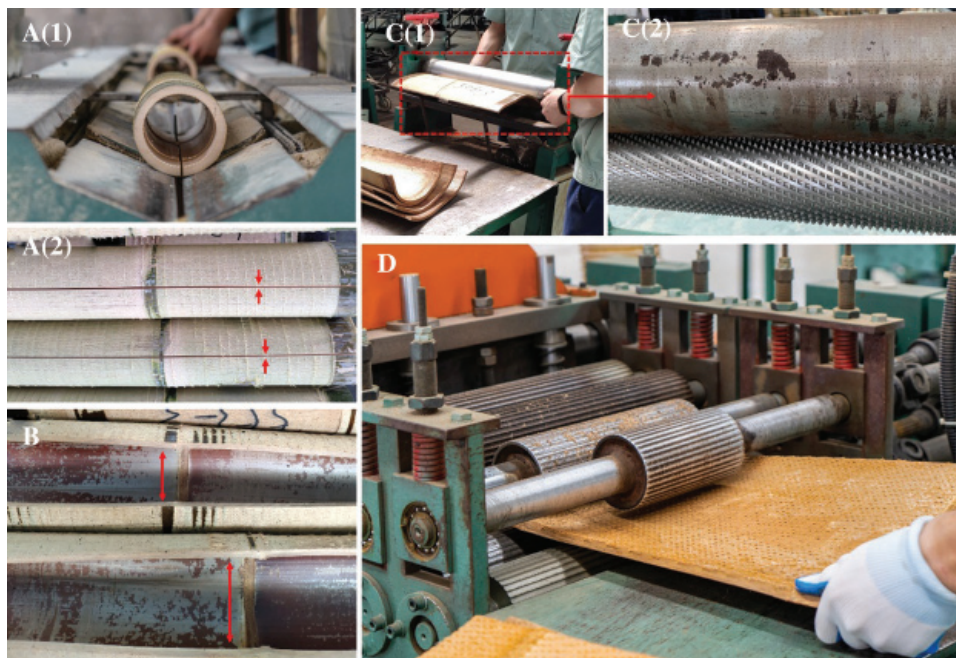


Figure 3: (A) Physical photos of slotting procedure (1) and slotted bamboo tubes (2). (B) physical photos of the slotted bamboo tubes after saturated steam heat treatment. (C) (1) Physical photo of the flattening processes of the bamboo tubes and (2) enlarged physical photo of the flattening roller with nails below. (D) Physical photo of cooling and shaping treatment

2.3 Characterization

2.3.1 X-Ray Diffraction (XRD) Analyses

X-ray diffract was used to evaluate crystallinity of bamboo tubes subjected to various treatments. Specifically, 200 mg of milled specimen powder was tested with a 2θ scanning range of $5^\circ\sim 40^\circ$ on a Bruker D8 Advance powder XRD machine operated at 40 kV and 40 mA using Cu-K α radiation ($\lambda = 1.54 \text{ \AA}$).

The corresponding relative crystallinities are calculated by the Segal formula [34]:

$$C_r = \left(\frac{I_{002} - I_{am}}{I_{002}} \right) \times 100\% \quad (1)$$

where C_r is the relative crystallinity (0–1), I_{002} is the maximum intensity of the 002 diffraction peak, and I_{am} is the non-crystalline diffraction intensity, which can be directly read by Jade 6.5.

2.3.2 Chemical Components Analyses

The chemical components (cellulose, hemicellulose and lignin) of the samples were determined by National Renewable Energy Laboratory (NREL) method as described previously [35]. The test was repeated five times for each sample and took the average value for the following discussion.

2.3.3 Color Analyses

The CIE-1976 L^* , a^* , and b^* standard chromaticity system was used to analyze the color of the samples, where L^* is the lightness value (0~100, 0 represents black, 100 represents perfect reflection of light), a^* is the red-green axis chromaticity index (-60~+60, -60 represents green, +60 represents red), and b^* is the yellow-blue axis chromaticity index (-60~+60, -60 represents blue, +60 represents yellow) [36]. The specimens were investigated by a colorimeter (CR-400, Konica Minolta from Japan). Each specimen was measured 10 times at 10 different points, and the obtained average values of L^* , a^* and b^* were collected.

The total color difference before and after treatment (ΔE^*) was calculated per the following equation:

$$\Delta E^* = \sqrt{(\Delta L^*)^2 + (\Delta a^*)^2 + (\Delta b^*)^2} \quad (2)$$

2.3.4 Physical, and Mechanical Testing of the Samples

Anti-expansion and shrinkage (AES) ability, bending strength and bending modulus of elasticity were investigated according to GB/T 15780-1995 (Testing methods for physical and mechanical properties of bamboo) national standard, utilizing an electronic universal testing machine (Model. UTM5105SLXY) from Shenzhen Suns Technology Stock Co., Ltd. The relative percent difference of these values between various treatment parameters was used to comprehend mechanical data.

2.3.5 Atomic Force Microscopy (AFM)

AFM was used to measure the micro morphology and micro mechanical properties of the samples. AFM imaging of the samples was performed in MFP-3D manufactured by Asylum Research. AC tapping mode was introduced to image the corresponding morphologies in air using a silicon nitride AFM tip with a curvature radius of 7 nm. Force spectroscopy was performed using a MFP-3D “closed loop” AFM system with a sensed piezo. Before acquiring force spectroscopy data, the AFM cantilever spring constant was calibrated through the resonance frequency changes which were induced by small mass. The cantilever spring constant of the tips used in this work was calibrated as 0.1 N/m. Young’s modulus was calculated using Hertz model:

$$F = \frac{4ER^{\frac{1}{2}}\delta^{\frac{3}{2}}}{3(1-\nu^2)} \quad (3)$$

where F is the loading force, ν is Poisson’s ratio (assumed to be 0.5), δ is the indentation depth, and E is the elastic modulus, R is the radius of the tip. Three different points were recorded from each scanning area, with each point being pressed 10–15 times in succession. Finally, the force-distance curves were assimilated and analyzed.

2.3.6 Scanning Electron Microscopy (SEM)

The corresponding morphologies of the samples which were firstly investigated by AFM, were then observed by SEM (Quanta 200, FEI). In details, we firstly found the area scanned by AFM in a large field of view, and then carried out SEM imaging with higher resolution.

3 Results and Discussions

A kind of bamboo veneer with practical application value, for consumers, mainly focuses on two aspects of performance, the first is physical and mechanical properties, the second is color. The former determines the quality of the veneer in the process of use, and the latter determines the decorative effect of the veneer in use. Based on this, we first studied the change rules of the above two properties of the board prepared under different softening process conditions. Then, through the study of the crystallinity and chemical composition, we reveal the change mechanism of the macro properties.

3.1 Physical and Mechanical Properties

The saturated steam heat treatment is very important to the flattening effect of bamboo tube. However, the saturated steam heat treatment process should affect the physical and mechanical properties of the treated board, and then affect the corresponding subsequent application. Considering this, we need to study the effect of saturated steam heat treatment on the physical and mechanical properties of treated board, so as to find out the appropriate treatment process parameters in actual industrial production.

3.1.1 AES Ability of Treated Bamboo Tubes

Figs. 4A and 4B show the air-drying and oven-drying AES rate of heat-treated bamboo tubes, respectively. It is obvious that under the same treatment temperatures, when treatment time is increased, the AES ability of the treated samples increases gradually. This indicates that more severe saturated steam heat treatments improve AES ability. However, dramatic improvement of air-drying AES capacity happens during the heat treatment time between 6 min and 8 min as shown in Fig. 4A, while that for oven-drying is between 4 min and 6 min.

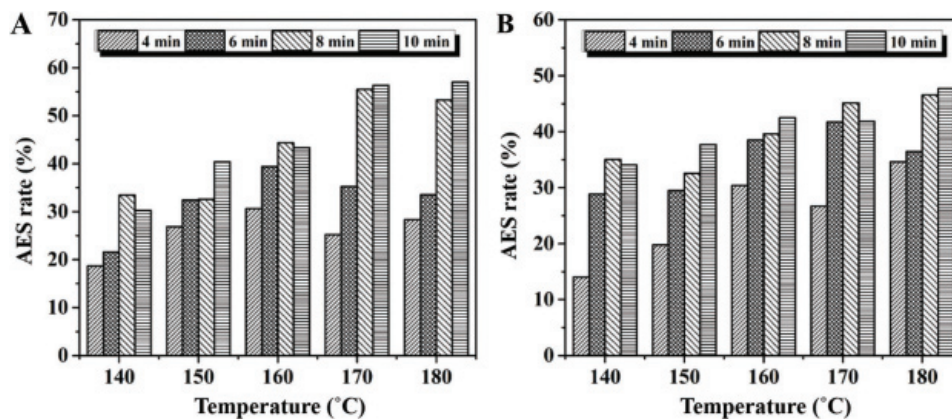


Figure 4: Air-drying (A) and oven-drying (B) anti-expansion and shrinkage (AES) rate of the treated samples

AES ability of all biomass-derived materials is closely related to its three major components. As discussed, the thermal fragility of hemicellulose relative to cellulose and lignin often comes into play when biomaterials are heat-treated. Previous work has shown that degradation of hemicellulose under high-temperature heat treatment is accompanied by loss of polysaccharide hydroxyl functionality [37]. This decrease is also correlated with improved AES ability. Fig. 5 shows the effects of heat treatment temperature and treatment time on the percentage of hemicellulose, cellulose and lignin of the treated bamboo tubes. It can be seen from Fig. 5A that hemicellulose content decreases with the increase of treatment temperature, from 23.5% (control) to 23.1% at 160°C and to 22.2% at 180°C. Furthermore, the relative content of cellulose is observed to decrease from 44.9% (control) to 44.5% at 160°C and to

44.0% at 180°C. This is attributed to the degradation of hemicellulose to produce acetic acid, which catalyzes degradation of amorphous cellulose. Finally, as hemicellulose and cellulose contents slightly decrease, the relative content of lignin increases from 31.6% (control) to 33.8% at 180°C. The same pattern can be seen when increasing reaction time (Fig. 5B).

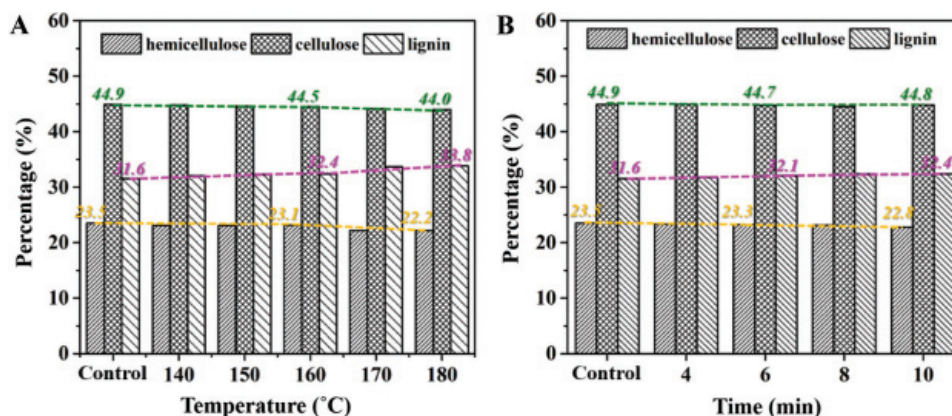


Figure 5: The relative contents of hemicellulose, cellulose and lignin in the samples obtained after saturated steam heat treatment over (A) constant time (8 min) and (B) constant temperature (160°C)

When comparing the wet material to its air-dried counterpart, the main difference is a decrease to the quantity of free water amongst the pores of the bamboo cells. Compared with air-dried treatment, oven-dried treatment is the removal of water molecules combined with cellulose hydroxyl groups via hydrogen bonding. With the increase of saturated steam heat treatment time, hemicellulose is degraded at first as shown in Fig. 5B, leading to the decrease of hydroxyl groups. As a result, between 4 min and 6 min, the AES capacity of treated samples increases between the wet sample and the oven-dried one. After further interaction, a large amount of steam enters into the gaps among the bamboo cell walls. However, the free water that was originally present becomes gasified, resulting in an increase to the internal porosity. This porosity buildup is more conducive to the entry of free water when these treated bamboo specimens are later introduced to moisture. Therefore, when the heat treatment time is 6–8 min, from wet samples to air-dried samples, the AES capacity of the treated samples increases dramatically. In addition, with the increase of saturated steam heat treatment temperature, the corresponding AES capacity increases, which is closely related to the degradation degree of hemicellulose as shown in Fig. 5.

3.1.2 Mechanical Properties of Heat-Treated Bamboo Tubes before Flattening

Fig. 6 shows the bending strength, modulus of elasticity, and corresponding relative percent difference after saturated steam heat treatment with different treatment temperatures and times. First, it can be seen on Fig. 6A that the bending strength of untreated bamboo tube is 120.5 MPa. Following saturated steam heat treatment, we see that bending strength slightly increased to 126.4 MPa when heated at 140°C at 4 min, translating to an ~5% increase. However, the bending strength of all other heat-treated materials decreased. Amongst those at constant steam temperature, bending strengths continually decrease. For the samples with constant heat treatment time, increasing temperature led to gradual reduction in bending strength. Finally, under the same treatment time, the higher the temperature is, the greater the reduction of bending strength is. Take for example the sample treated at 180°C for 10 min, which showed a 36.22% decrease in bending strength. The least affected sample with respect to bending strength was that which was treated at 140°C for 6 min, is the smallest, only 0.91% decrease. Such decrease of bending strength

of treated bamboo tubes is likely most driven by the previously discussed degradation of hemicellulose. In this case, its degradation renders bamboo more brittle as evidence from the decrease to bending strength.

Figs. 6C and 6D show the modulus of elasticity of bamboo tubes after saturated steam heat treatment at both constant temperature or constant treatment time. It can be seen in Fig. 6C that, except for 180°C, elasticity moduli first increase but then decrease at prolonged treatment time. It is worth noting that, for the temperatures of 140°C and 150°C, saturated steam heat treatment appears helpful for elasticity moduli. Specifically, the elastic modulus of these samples increased by 21.2%, 21.7%, 22.1% and 20.9% after being treated for 4–10 min at 140°C, and by 13.3%, 10.1% and 5.7% respectively after being treated for 4-8 min at 150°C. Only when treated at 150°C for 10 min did the bending modulus begin to slightly decrease by an extent of 1.2%. For temperatures below 140°C, the increase of elastic moduli could be due to loss of free water in the amorphous regions of cellulose. This would provide a closer arrangement of cellulose molecular chains. Since the relative content of cellulose increases with the softening reactions as shown in Fig. 5, the corresponding molecular crystallinity should increase. As a result, the corresponding elastic moduli increases. This can be proved by the XRD results of these treated samples.

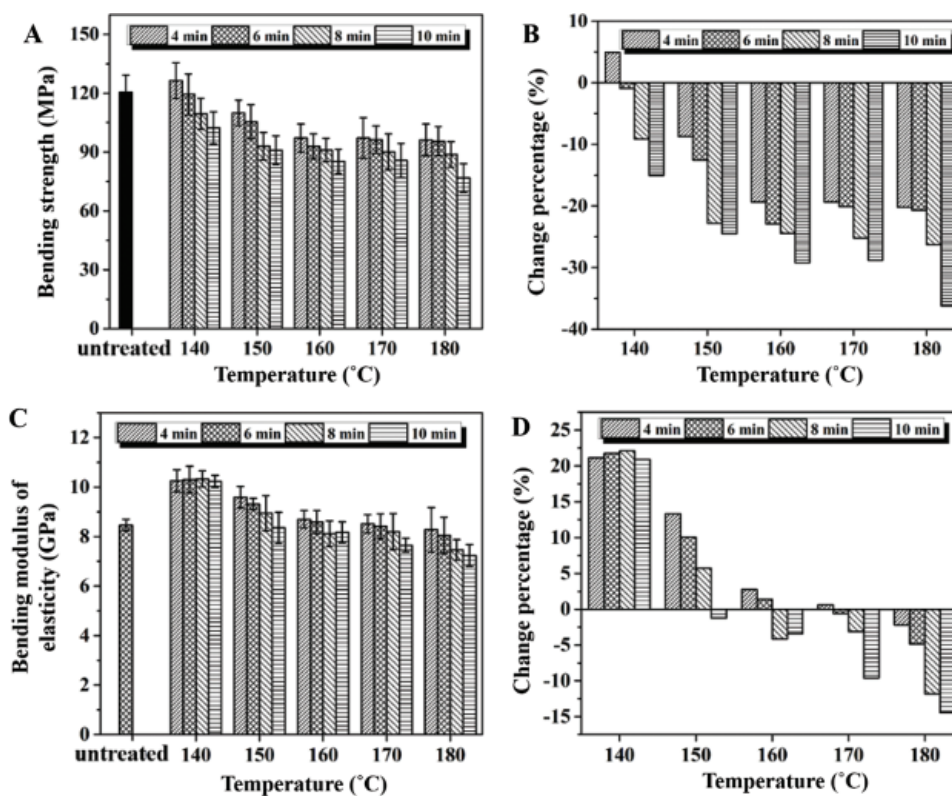


Figure 6: (A, B) Bending strength of the samples and the corresponding relative percent difference compared with untreated sample. (C, D) Bending elastic modulus of the samples and corresponding relative percent difference compared with untreated sample

Figs. 7A and 7B show XRD curves of the bamboo tubes after saturated steam heat treatment at constant time and constant temperature. The diffractograms of the treated samples show a pattern quite similar with the three primary diffraction peaks characteristic of untreated bamboo (cellulose I). These peaks are approximately located at 16°, 22° and 35°, which represent the characteristic peaks produced by the amorphous state with (101) and (10 $\bar{1}$) crystal planes, the cellulose (002) and (040) crystallographic plane

reflections, respectively [38,39]. The lack of differentiation between samples at this peak indicates that the saturated steam heat treatment provided no obvious effect on the crystalline regions within bamboo. However, the corresponding exact (002) diffraction peak positions and the relative crystallinities are listed in Tab. 1. It can be seen from Tab. 1 that the positions of the (002) diffraction peaks of the treated samples are all in the range of 21.74–22.04°, which are lower than those of untreated bamboo tubes (22.06°). This is perhaps attributable to saturated steam heat treatment introducing macroscopic residual stress inside the cellulose's crystalline regions, resulting in the distortion of crystal lattices. As a result, the corresponding lattice anisotropy increases, crystal spacing became larger, and the diffraction peak decreased [40]. It is obvious that the relative crystallinities of all the treated samples are larger than that of untreated bamboo tube (49.7%), indicating that saturated steam heat treatment worked towards elevating overall crystallinity of bamboo cellulose. As we know, biomass cellulose contains quasi crystalline regions. The observed increase in crystallinity may be due to the crystallization in these amorphous regions, being attributed to rearrangement or reorientation of cellulose molecules inside these regions [41]. Besides, there are evidences that thermal stability of amorphous cellulose in the quasi crystalline region is poor. Therefore, in the present study, in addition to crystallization in quasi crystalline regions, the degradation of cellulose in the amorphous region may happen at high temperature, which results in more crystallization [42]. For example, the corresponding relative crystallinity increases from 53.2 to 54.6 with the increase of treatment time from 4 min to 10 min at 160°C. However, under the same treatment time (8 min), with the increase of temperature, the relative crystallinity increased first, then decreased, and finally increased again. This could be due to the lignin remaining chemically stable under the conditions of heat treatment. Conversely, the thermal stability of hemicellulose is the lowest among bamboo's constituent polymers, so its degradation occurs first at high temperatures (Fig. 5A). The increase of relative crystallinity is therefore most likely attributed to the hemicellulose destruction. On the other hand, acetic acid byproducts formed via destruction hemicellulose can catalyze the hydrolysis of cellulose's amorphous regions. If this is taking place, then additional ode for increasing crystallinity is expected. When temperature was further increased, the hemicellulose degradation processes are dominant, which makes the relative crystallinity further improved.

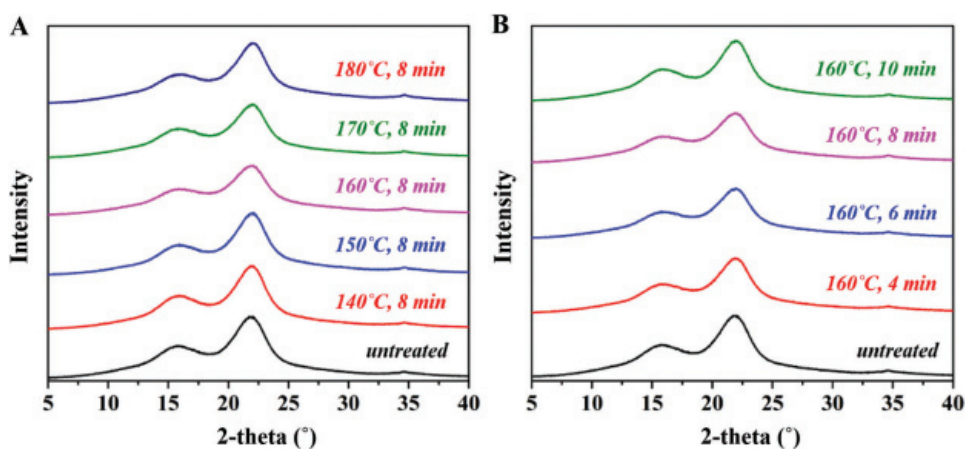


Figure 7: XRD curves of bamboo tubes after saturated steam heat treatment over (A) constant time (8 min) and (B) constant temperature (160°C)

For samples treated at temperatures between 160 and 180°C, the elastic moduli decrease dramatically (Fig. 6D). We believe that this decrease is mainly due to the acetic acid cleaved from hemicellulose during its degradation (Fig. 5), which can catalyze some degradation of cellulose at higher temperatures

leading to a reduction in crystallinity (as shown in [Tab. 1](#)). At the same time, some physical and perhaps even chemical connections between biomass' constituent polymers can be severed under higher steam pressures. This can drive formation of a physical split of intercellular layers, reducing the mechanical properties evaluated in this work.

Table 1: Summary of the (002) peak position and relative crystallinities obtained according to the XRD curves of the samples tested in [Fig. 3](#)

| Temperature (°C) | Time (min) | (002) peak position (°) | relative crystallinities (%) |
|------------------|------------|-------------------------|------------------------------|
| 140 | 8 | 21.84 | 56.0 |
| 150 | | 22.04 | 56.6 |
| 160 | | 21.94 | 54.0 |
| 170 | | 21.94 | 55.0 |
| 180 | | 22.04 | 55.6 |
| 160 | 4 | 21.86 | 53.2 |
| | 6 | 21.74 | 53.9 |
| | 8 | 21.94 | 54.0 |
| | 10 | 22.00 | 54.6 |
| Control | | 22.06 | 49.7 |

3.1.3 Macro-Mechanical Properties of the Heat-Treated Bamboo Tube After Flattening

Bending strength and elastic moduli of flattened bamboo boards are listed in [Tab. 2](#). It can be seen from [Tab. 2](#) that, compared with the samples before flattening, the corresponding mechanical properties of most samples was reduced to various extents. This is mainly because the flattening process exert significant stress onto the bamboo and cause further physical degradation. This stress comes from the nails adorning the roller, which penetrate into the inner surface of bamboo tubes and flatten or even crush surrounding thin-walled cells. However, the flattened bamboo samples produced from bamboo tubes treated at 160°C for 8 min appear to be an exception. Specifically, the corresponding bending strengths after flattening for these samples was larger than before flattening, although the bending modulus still decreased. Moreover, compared with all the flattened materials in [Tab. 2](#), the flattened bamboo samples with saturated steam heat treatment at 160°C for 8 min exhibited excellent macro-mechanical performance. Considering this subset of samples, we already know that there is degradation of hemicellulose and loss of hydroxyl groups ([Fig. 5](#)). 160°C and 8 min should be the optimal softening process parameter for practical production.

Table 2: Summarization of the bending strength and bending modulus of the samples after flattening

| | Time (min) | Temperature (°C) | | | | |
|------------------------|------------|------------------|-------|-------|-------|------|
| | | 140 | 150 | 160 | 170 | 180 |
| Bending strength (MPa) | 4 | 110.5 | 106.3 | 112.4 | 109.5 | 96.9 |
| | 6 | 97.7 | 92.5 | 109.6 | 101.8 | 92.8 |
| | 8 | 80.3 | 88.4 | 101.5 | 87.0 | 87.2 |
| | 10 | 77.0 | 81.4 | 94.7 | 77.3 | 86.4 |

(Continued)

Table 2 (continued).

| | Time (min) | Temperature (°C) | | | | |
|-----------------------|------------|------------------|-----|-----|-----|-----|
| | | 140 | 150 | 160 | 170 | 180 |
| Bending modulus (GPa) | 4 | 4.6 | 5.6 | 5.3 | 8.4 | 6.9 |
| | 6 | 5.8 | 5.9 | 6.1 | 7.4 | 6.8 |
| | 8 | 5.9 | 5.7 | 7.7 | 7.0 | 6.2 |
| | 10 | 7.7 | 7.4 | 6.9 | 6.8 | 6.0 |

3.2 Color Testing of Bamboo Tubes

With the improvement of living conditions of human beings, people's demand for the color of decorative and building materials grows richer. Some pursue the natural colorations of bright yellow bamboo, whilst others appreciate the darker colors of processed materials. By treating bamboo in high temperature in advance, the brightness and shade of the bamboo color can be adjusted, but at the same time, the color changes in the red-green and yellow-blue spectra.

L^* value (0–100) stands for lightness, 0 for black and 100 for perfect reflection of light. The changing trend of L^* values of the treated bamboo tubes after removal of outer and inner surfaces is shown in Fig. 8A. It is obvious that under different saturated steam heat treatment temperature, L^* values decrease with the increase of treatment time. Under the same heat treatment time, L^* values also decreased with the increase of treatment temperature. As a result, the color of bamboo tubes becomes black and dark after saturated steam heat treatment. Sources of color in biomaterials include carbonyls ($=C=O$), carboxyls ($-COOH$), olefins ($C=C$), conjugated chromophores, hydroxyls ($-OH$), and other auxochrome groups. It is important to note that the majority of these structures are present in the lignin fraction, therefore close consideration must be paid to how lignin behaves during heat treatment in order to control color properties. As shown in Fig. 5, while contents of cellulose and hemicellulose decrease with increasing steam temperature, the quantities of carbonyl and carboxyl groups conversely rise. At the same time, the relative content of lignin increases, leading to the color change from bright yellow to dark brown [43]. Regarding a^* , representing the red-green index, no consistent patterns are observed (Fig. 8B). This suggests that heat treatment has no effect on this color spectrum. However, a trend was observable for the b^* value (blue-yellow index), and it appears that the color of the treated samples tends to gradually become more blue. Finally, it can be seen from Fig. 8D that with the increase of saturated steam heat treatment time, ΔE^* values increase. These results indicate that the difference between the color of treated and untreated bamboo tubes becomes greater. This changing trend is consistent with that of wood when it is similarly heat treated. This suggests that the change of bamboo color during heat treatment is mainly caused by changes to chemical composition [44]. Since both L^* and b^* decrease with the extension of reaction time, which is contrary to the change trend of ΔE^* , while a^* exhibits no regular changing trend with the increase of reaction time, we can conclude according to Eq. (2) that the change of ΔE^* mainly depends on the change of L^* and b^* .

In effort to understand how to control the color changes, the most influenced color changes (a^* and b^*) against recorded L^* values are plotted in Fig. 9. A compilation of the obtained correlations is shown in Fig. 9. First, it can be seen that with the decrease of bamboo brightness, a^* and b^* both show a linear decrease. However, both metrics remain greater than 0, indicating the treated bamboo tubes display reddish yellow. Without considering the treatment temperature and time, the maximum value of a^* and b^* is obtained as 9.76 and 20.77 with L^* value of 44.86 and 55.45, respectively. Furthermore, the degree of change for b^* is shown to be larger than a^* at a fixed temperature. When the temperatures were 140°C and 150°C, L^* values of the treated bamboo tubes remained in the range of 48–64. However, when the temperature

increased from 160°C up to 180°C, the corresponding adjustable range reduced to 44–56 and to 24–48, respectively. Different from L^* value, the adjustable range of b^* value is not affected by the treatment temperature when lower temperatures are applied. For example, as shown in Figs. 9A–9D, the b^* value is kept in the range of 12–24 between 140°C and 170°C. However, when the temperature is further increased to 180°C (Fig. 9E), the adjustable range of b^* value is reduced to 4–16. Compared with L^* and b^* values, the adjustable range of a^* remains at 4–8.

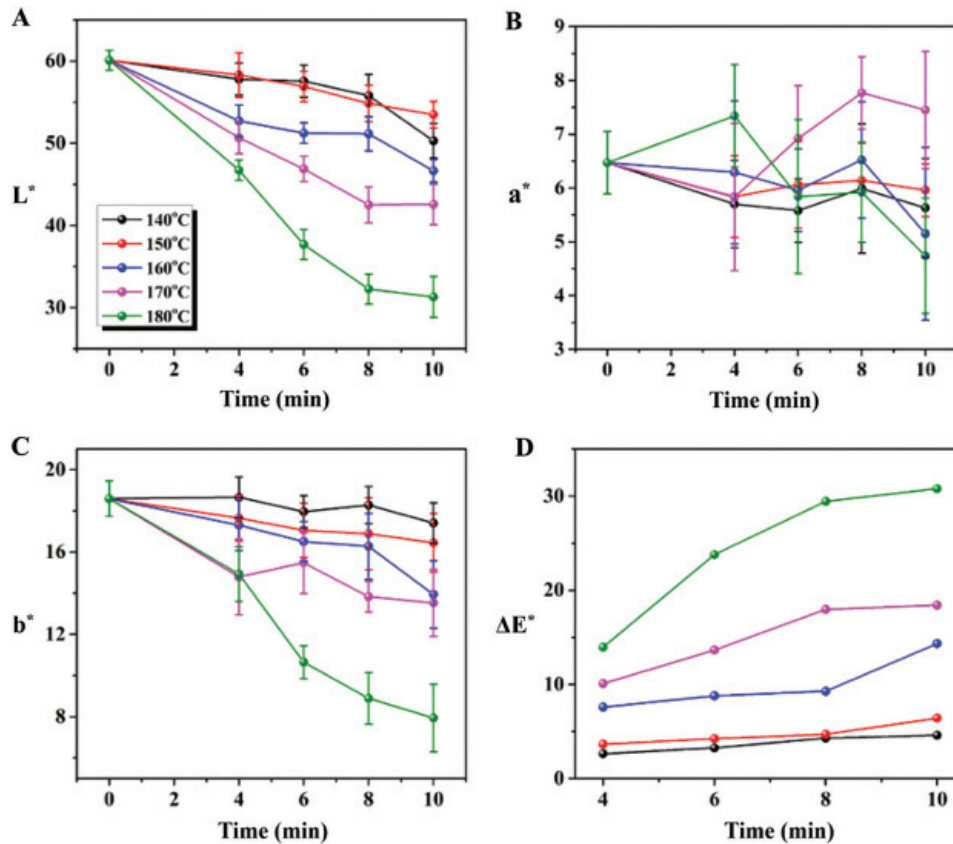


Figure 8: (A) L^* , (B) a^* , (C) b^* , and (D) ΔE^* values of the obtained sample colors

3.3 Micromorphology and Micromechanics of the Samples

SEM and AFM imaging were next used to investigate the micromorphology and micromechanics of bamboo samples before and after flattening. The only samples imaged were those steam-treated at 160°C for 8 min, in effort to better understand the micro mechanism of mechanical properties change before and after flattening procedure. Fig. 10 shows the micro-morphologies of cross sections for these bamboo samples, along with the force spectroscopy data of corresponding conduit walls. It is obvious from Figs. 10A and 10B(1–2) that the cross section of bamboo samples before flattening processes is full of plump, round pores consisting of bamboo fibers and vascular bundles. It can be observed from the *in-situ* AFM cross-section file in Fig. 10B(2) that the height of the conduit wall reaches as high as 6.67 μm which is due to the presence of adjacent pores. The obtained Young's modulus of the conduit wall in radial direction (YR) is calculated as 3.48 GPa from the force-distance curves in Fig. 10B(3). However, after flattening, obvious nail holes with diameters larger than 1 mm are observed in Fig. 10C(1), which are produced by the nails in the flattening machine as shown in Fig. 7C(2). It can be seen from the enlarged SEM image (Fig. 10C(2)) that the bamboo fiber at the nail hole was torn and exposed

completely. Meanwhile, there were no porous structures observed after the rolling process, as shown in Fig. 10C(3). This is due to the direction by which the bamboo is compressed, from the inside to the outside. Normally destruction of porous structural characteristics and the compactness of texture are conducive to improvements in rigidity and loss of toughness for biomass materials [45]. Therefore, the results found in these images were not necessarily surprising.

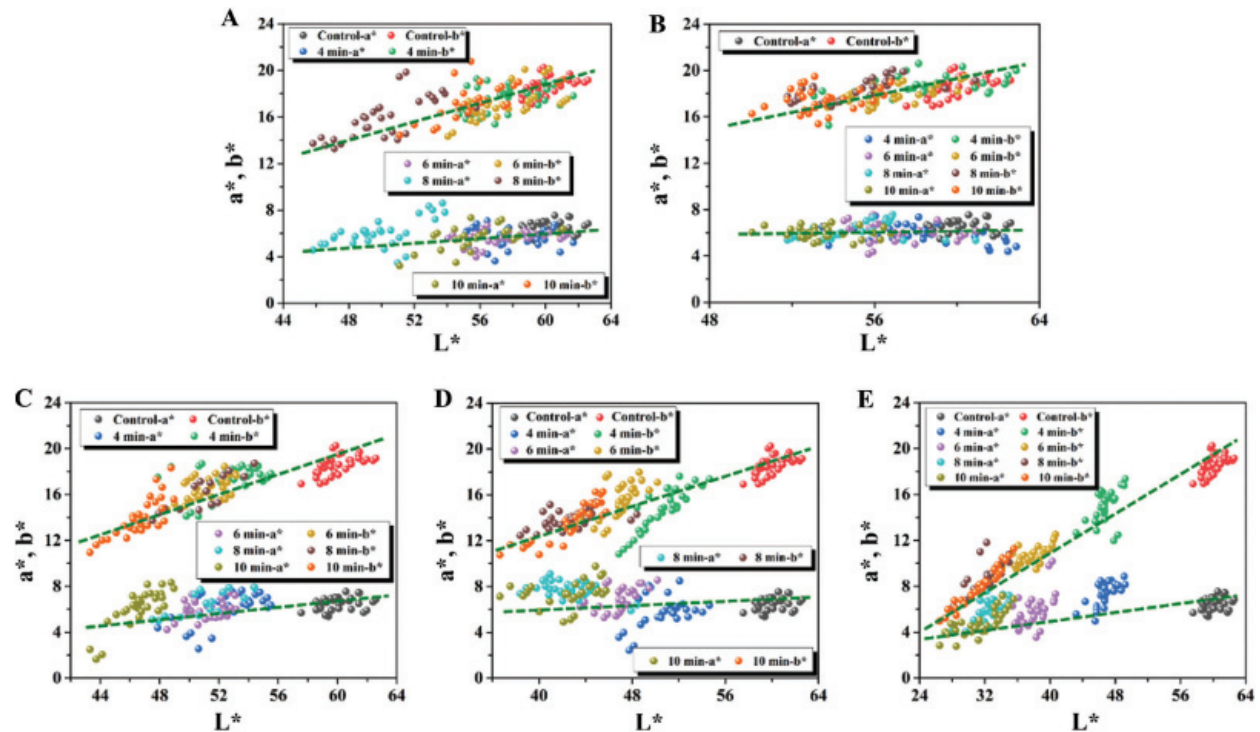


Figure 9: Relationship between a^* and b^* coordinates and L^* in heat-treated bamboo tubes obtained at (A) 140°C, (B) 150°C, (C) 160°C, (D) 170°C and (E) 180°C with different treatment times of 4, 6, 8 and 10 min

In-situ high-resolution AFM technology was used to observe the micromorphology of the flattened bamboo cross-section in Fig. 10D(1–2). It was found in these images that although the original porous structure was changed into a continuous plane (Fig. 10D(1)), in the AFM image with $10 \times 10 \mu\text{m}$ area in Fig. 10D(2), the conduit walls are observed to be broken into smaller pieces that are squeezed and stacked together. These pieces appear to have formed small discontinuous cracks with a diameter of $\sim 1 \mu\text{m}$. In other words, the original regular porous structures of the bamboo cross sections underwent structural collapse hence the observed decline of the corresponding rigidity and toughness. Furthermore, calculated YR value of the densified cross section increases to 7.29 GPa according to the force curves in Fig. 10D(3). This value is larger than what was measured for the conduit walls of bamboo prior to flattening. The increase is attributed to the hydrogen bonding interactions between the exposed hydroxyl groups from the microcrystalline cellulose on the surface of the conduit walls, which improves the rigidity of bamboo in the radial direction.

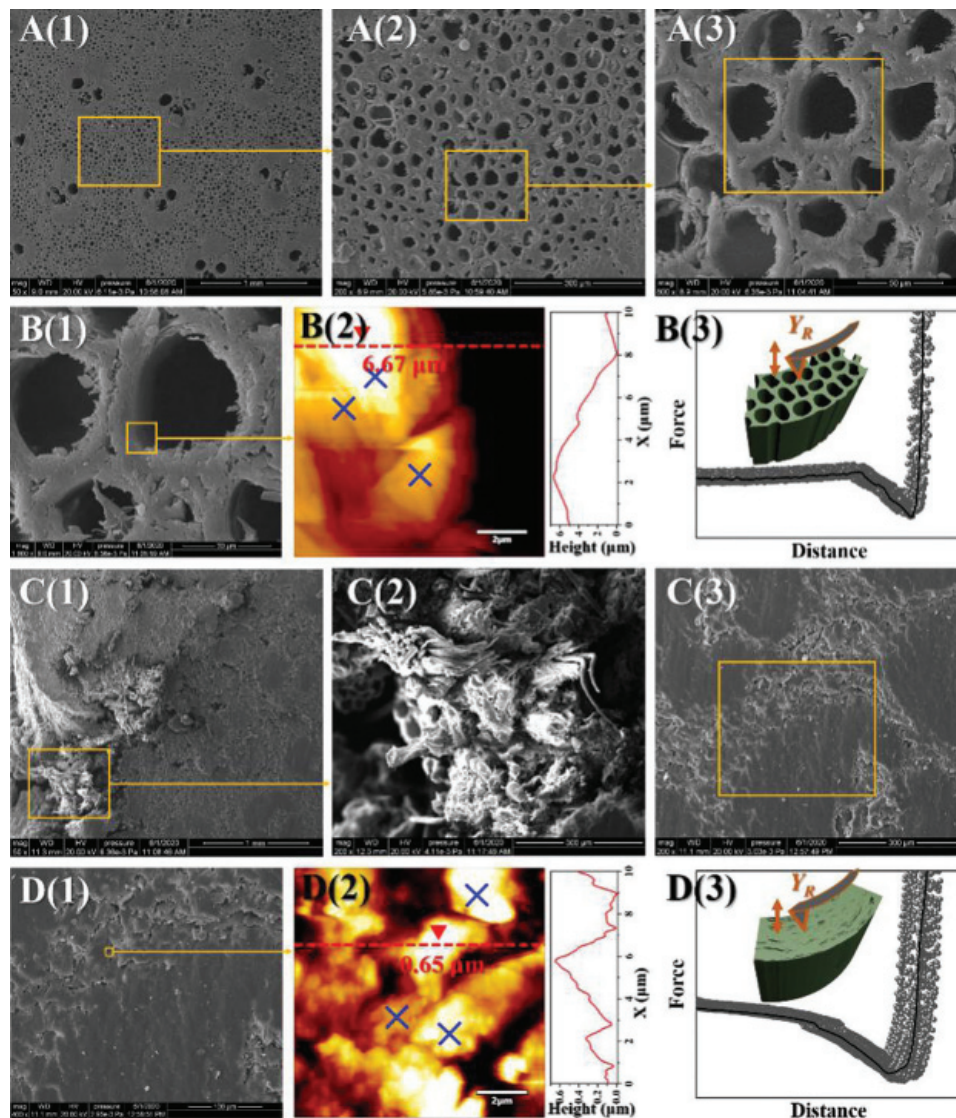


Figure 10: (A and C) (1-3) SEM images of cross-sections of bamboo before and after flattening at different magnifications. (B and D) *In-situ* (1) SEM and (2) AFM images, along with the corresponding AFM cross-section profile, (3) force-distance curves of AFM force spectroscopy following the radial direction for bamboo before and after flattening bamboo. Blue '×' represents the pressing points of AFM tips

Fig. 11 contains images of micro-morphologies present in the radial sections of bamboo samples, along with force spectroscopy data from corresponding conduit walls. As shown in Fig. 11A, the cavities of bamboo fiber cells are full and regular. It is obvious that the profile of fiber cells of unflattened bamboo is stereoscopic, and the height of the 1/2 profile is determined as $6.83 \mu\text{m}$ according to the AFM cross-section profile in Fig. 11B(2). Based on the force-distance curves obtained by AFM force spectroscopy in Fig. 11B(3), the Young's modulus of the cell membrane in transverse direction (YT) was 1.48 GPa. SEM images of radial sections of flattened bamboo are in Fig. 11C(1–3). The trace left by the nails after rolling is obvious in Fig. 11C(1). From the enlarged SEM images in Figs. 11C(2) and 11C(3), it can be seen that the fiber cells of the flattened bamboo are completely compressed and flattened and loss the original stereoscopic sense as shown in Fig. 11A. This is consistent with the phenomenon observed on the cross-section in Fig. 10. Meanwhile, the cell walls are observed to be seriously fragmented, and almost no full cell cavity is observed in Fig. 11C(2–3). Fig. 11D(1–2) show the *in-situ* SEM and AFM images, as well

as the corresponding AFM cross-section profile. It can be seen that the thickness of bamboo fiber cells after flattening processes is only $1.62\ \mu\text{m}$, much lower than that bamboo cells without flattening. This differential again points to crushing of bamboo fiber cells during flattening. At the same time, bamboo cells on the inner surface are affected by lateral stretching. Such changes in morphology also explains the reason for the observed improvement of bending strength. The contact area between the stretched flat cell membrane is larger than that of full cells, which makes it easier for them to form hydrogen bonds between cellulose hydroxyl groups on the cell membrane surface. The formation of a large number of hydrogen bonds is conducive to the improvement of mechanical properties. The resulted YT value is calculated as $1.00\ \text{GPa}$, which is lower than that of unflatten bamboo samples, and is consistent with the reduction of the micro bending modulus as shown in Fig. 6C and Tab. 2.

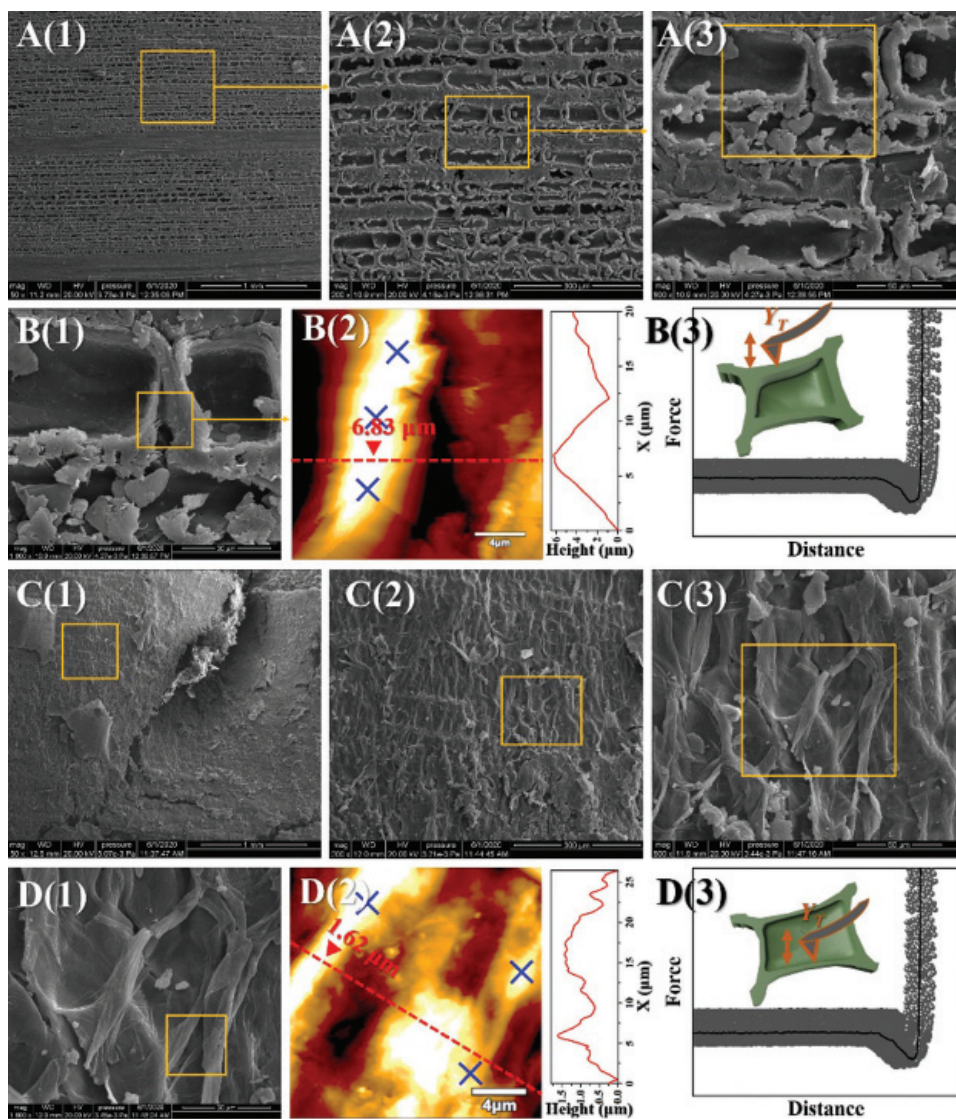


Figure 11: (A and C) (1–3) SEM images of the radial-sections of bamboo before and after flattening at different magnifications. (B and D) *In-situ* (1) SEM and (2) AFM images, along with the corresponding AFM cross-section profile, (3) force-distance curves of AFM force spectroscopy following transverse direction for unflatten bamboo and flattened bamboo, respectively. The blue ‘x’ represents the pressing points of AFM tips

4 Conclusions

Herein, crack-free flattened bamboo boards were fabricated by flattening both softened and slotted bamboo tubes with a roller device with nails. The chemical and physical properties, as well as mechanical properties of the samples obtained after softening processes and flattening processes, were tested. The relative contents of the components, such as non-crystalline cellulose and hemicellulose, were found to decrease while the relative content of lignin increased after the saturated steam heat treatment. As a result, the color of the heated bamboo tubes turned into dark blue, and the relative crystallinity and AES capacity increased. All these changes are attributed to the degradation of hemicellulose and cellulose in amorphous region, rearrangement or reorientation of cellulose in crystalline area, and the thermal stability of lignin. Flattened bamboo boards were shown to possess an increased bending strength of 101.5 MPa and a decreased bending modulus of 7.7 GPa compared with only-softened bamboo tubes. The optimal softening parameters for saturated steam heat treatment is proved to be 160°C for 8 minutes. Samples produced under these conditions were then analyzed by the micro-morphological and mechanical techniques in order to explain their superiority. It is concluded that the action of nails presents on the rolling apparatus compacted the crushed and fragmented conduit walls present. The cell cavities left by this compacted material became stretched and compressed after flattening, allowing for the process to overcome any mechanical penalties otherwise associated with the flattening operation. Our work provides a possibility to develop round bamboo tubes into crack-free bamboo boards assuming an optimal softening process is discovered for each process. Furthermore, these results help to lay a theoretical and experimental foundation for efficient and high-added value utilization of bamboo as a biomaterial.

Funding Statement: This research was funded by Financial support from the National Natural Science Foundation of China (Nos. 61601227, 31971740), China Postdoctoral Science Foundation (2017M621598), Nature Science Foundation of Jiangsu Province (BK20160939), Key University Science Research Project of Jiangsu Province (17KJA220004), Jiangsu Agricultural Science and Technology Independent Innovation Project (CX(18)3033), Science and Technology Program of Fujian Province (2019N3014), Open Fund of Key Laboratory of National Forestry and Grassland Administration/Beijing for Bamboo & Rattan Science and Technology (ICBR-2020-08).

Conflicts of Interest: The authors declare that they have no conflicts of interest to report regarding the present study.

References

1. Zhao, W., Luo, Z., Li, Y. (2020). Axial compression testing of bamboo–laminated encased steel tube composite columns. *Iranian Journal of Science and Technology*, 44, 645–655.
2. Li, H. T., Qiu, Z. Y., Wu, G., Wei, D. D., Lorenzo, R. et al. (2019). Compression behaviors of parallel bamboo strand lumber under static loading. *Journal of Renewable Materials*, 7(7), 583–600. DOI 10.32604/jrm.2019.07592.
3. Hong, C. K., Li, H. T., Xiong, Z. H., Lorenzo, R., Corbi, I. et al. (2020). Review of connections for engineered bamboo structures. *Journal of Building Engineering*, 30, 101324. DOI 10.1016/j.job.2020.101324.
4. Li, J., Xu, B., Zhang, Q., Jiang, S. (2016). Present situation and the countermeasure analysis of bamboo timber processing industry in China. *Journal of Forestry Engineering*, 1, 2–7.
5. Huang, Y. X., Qi, Y., Zhang, Y. H., Yu, W. J. (2019). Progress of bamboo recombination technology in China. *Advances in Polymer Technology*, 2019(4), 1. DOI 10.1155/2019/2723191.
6. Mahdavi, M., Clouston, P. L., Arwade, S. R. (2011). Development of laminated bamboo lumber: Review of processing, performance, and economical considerations. *Journal of Materials in Civil Engineering*, 23(7), 1036–1042. DOI 10.1061/(ASCE)MT.1943-5533.0000253.
7. Khalil, H. P. S. A., Bhat, I. U. H., Jawaid, M., Zaidon, A., Hermawan, D. et al. (2012). Bamboo fibre reinforced biocomposites: A review. *Materials & Design*, 42, 353–368. DOI 10.1016/j.matdes.2012.06.015.

8. Zhang, Q. (1988). Studies of bamboo plywood–I. The softening and flattening of bamboo. *Journal of Nanjing Forestry University (Natural Science Edition)*, 12, 13–20.
9. Li, Y. J., Lou, Z. C., Jiang, Y. J., Wang, X. Z., Yuan, T. C. et al. (2020). Flattening technique without nicked in curved bamboo strips. *Forestry Machinery & Woodworking Equipment*, 48, 28–30+34.
10. Xiao, Y., Yang, R. Z., Shan, B. (2013). Production, environmental impact and mechanical properties of glulam. *Construction and Building Materials*, 44, 765–773. DOI 10.1016/j.conbuildmat.2013.03.087.
11. Luan, F. (2007). Flattening technology and equipment of bamboo sheet. *Forestry Machinery & Woodworking Equipment*, 35, 51–52.
12. Jiang, S. (1995). The study of bamboo piece softening machine with conveying chain. *Journal of Nanjing Forestry University (Natural Science Edition)*, 19, 53–58.
13. Liu, H. Z., Wang, X. Z., Li, Y. J., Xu, B., Chen, L. C. et al. (2018). Manufacturing technique of crack-free flattened bamboo tube. *China Forest Products Industry*, 45, 40–44.
14. Zhao, Z. (2015). Patent analysis of bamboo flattening. *Agricultural Development and Equipments*, 7, 51.
15. Huang, M., Zhang, W., Zhang, X., Li, W., Yu, W. et al. (2015). Advances in bamboo softening and flattening technology. *Journal of Bamboo Research*, 34, 31–36.
16. Wang, Q., Wu, X., Yuan, C., Lou, Z., Li, Y. (2020). Effect of saturated steam heat treatment on physical and chemical properties of bamboo. *Molecules (Basel, Switzerland)*, 25, 1999.
17. Placet, V., Passard, J. B., Perré, P. (2008). Viscoelastic properties of wood across the grain measured under water-saturated conditions up to 135°C: Evidence of thermal degradation. *Journal of Materials Science*, 43(9), 3210–3217. DOI 10.1007/s10853-008-2546-9.
18. Lou, Z., Yuan, C., Li, Y., Shen, D., Yang, L. et al. (2020). Effect of saturated steam treatment on the chemical composition and crystallinity properties of bamboo bundles. *Journal of Forestry Engineering*, 5, 29–35.
19. Zhang, X. C., Zhou, Z. Z., Zhu, Y. D., Dai, J. F., Yu, Y. M. et al. (2019). High-pressure steam: a facile strategy for the scalable fabrication of flattened bamboo biomass. *Industrial Crops and Products*, 129, 97–104. DOI 10.1016/j.indcrop.2018.11.061.
20. Li, Y., Hu, S., Lv, R., Zhang, A., Liu, H. et al. (2018). Production technology of outdoor reconstituted bamboo. *China Wood-Based Panels*, 25, 9–13.
21. Song, L., Ren, H., Wang, X., Ma, J., Li, Y. et al. (2018). Effect of high temperature saturated steam treatment on bamboo properties. *Journal of Forestry Engineering*, 3, 23–28.
22. Azadeh, A., Ghavami, K. (2018). The influence of heat on shrinkage and water absorption of *Dendrocalamus giganteus* bamboo as a functionally graded material. *Construction and Building Materials*, 186, 145–154. DOI 10.1016/j.conbuildmat.2018.07.011.
23. Nguyen, Q. T., Nguyen, T., Nguyen, N. (2019). Effects of bleaching and heat treatments on *Indosasa angustata* bamboo in Vietnam. *BioResources*, 14, 6608–6618.
24. Akerholm, M., Salmen, L. (2003). The oriented structure of lignin and its viscoelastic properties studied by static and dynamic FT-IR spectroscopy. *Holzforschung*, 57(5), 459–465. DOI 10.1515/HF.2003.069.
25. Matan, N., Kyokong, B., Preechatiwong, W. (2011). Softening behavior of black sweet-bamboo (*Dendrocalamus asper* Backer) at various initial moisture contents. *Walailak Journal of Science and Technology (WJST)*, 4, 225–236.
26. Liu, Z., Jiang, Z., Cai, Z., Fei, B., Yu, Y. et al. (2012). Dynamic mechanical thermal analysis of moso bamboo (*Phyllostachys heterocycla*) at different moisture content. *Bioresources*, 7, 1548–1557.
27. Zhang, Y. M., Yu, Y. L., Yu, W. J. (2013). Effect of thermal treatment on the physical and mechanical properties of *Phyllostachys pubescens* bamboo. *European Journal of Wood and Wood Products*, 71(1), 61–67. DOI 10.1007/s00107-012-0643-6.
28. Wang, J. S., Demartino, C., Xiao, Y., Li, Y. Y. (2018). Thermal insulation performance of bamboo- and wood-based shear walls in light-frame buildings. *Energy and Buildings*, 168, 167–179. DOI 10.1016/j.enbuild.2018.03.017.

29. Mahdavi, M., Clouston, P. L., Arwade, S. R. (2011). Development of laminated bamboo lumber: Review of processing, performance, and economical considerations. *Journal of Materials in Civil Engineering*, 23(7), 1036–1042. DOI 10.1061/(ASCE)MT.1943-5533.0000253.
30. Quaranta, G., Demartino, C., Xiao, Y. (2019). Experimental dynamic characterization of a new composite glulam-steel truss structure. *Journal of Building Engineering*, 25, 100773. DOI 10.1016/j.jobbe.2019.100773.
31. Xiao, Y., Zhou, Q., Shan, B. (2010). Design and construction of modern bamboo bridges. *Journal of Bridge Engineering*, 15(5), 533–541. DOI 10.1061/(ASCE)BE.1943-5592.0000089.
32. Li, Y. J., Xu, B., Zhang, Q. S. (2018). A process method of removing the outer and inner layers of bamboo tubes, Patent ZL201610198832.8, China.
33. Li, Y. J., Wang, X. Z., Shao, Y. T., Song, B. Q. (2019). A kind of floating machine for removing the outer layer of bamboo. Patent ZL210414879U, China.
34. Dalmis, R., Koktas, S., Seki, Y., Kilinc, A. C. (2020). Characterization of a new natural cellulose based fiber from Hierochloe Odarata. *Cellulose*, 27(1), 127–139. DOI 10.1007/s10570-019-02779-1.
35. Lin, W., Xing, S., Jin, Y., Lu, X., Huang, C. et al. (2020). Insight into understanding the performance of deep eutectic solvent pretreatment on improving enzymatic digestibility of bamboo residues. *Bioresource Technology*, 306, 123163. DOI 10.1016/j.biortech.2020.123163.
36. Thompson, D. W., Kozak, R. A., Evans, P. D. (2005). Thermal modification of color in red alder veneer. I. Effects of temperature, heating time, and wood type. *Wood and Fiber Science*, 37, 653–661.
37. Wang, X. Z., Cheng, D. L., Huang, X. N., Song, L. L., Gu, W. L. et al. (2020). Effect of high-temperature saturated steam treatment on the physical, chemical, and mechanical properties of moso bamboo. *Journal of Wood Science*, 66(1), 52. DOI 10.1186/s10086-020-01899-8.
38. El Oudiani, A., Chaabouni, Y., Msahli, S., Saldi, F. (2011). Crystal transition from cellulose I to cellulose II in NaOH treated Agave americana L. fibre. *Carbohydrate Polymers*, 86(3), 1221–1229. DOI 10.1016/j.carbpol.2011.06.037.
39. Khalifa B. A., Abdel-Zaher N., Shoukr F. S. (2016). Crystalline character of native and chemically treated Saudi Arabian cotton fibers. *Textile Research Journal*, 61(10), 602–608. DOI 10.1177/004051759106101007.
40. Okon, K. E., Lin, F., Chen, Y., Huang, B. (2017). Effect of silicone oil heat treatment on the chemical composition, cellulose crystalline structure and contact angle of Chinese parasol wood. *Carbohydrate Polymers*, 164, 179–185. DOI 10.1016/j.carbpol.2017.01.076.
41. Lorenzo, R., Godina, M., Mimendi, L., Li, H. T. (2020). Determination of the physical and mechanical properties of moso, guadua and oldhamii bamboo assisted by robotic fabrication. *Journal of Wood Science*, 66(1), 40. DOI 10.1186/s10086-020-01869-0.
42. Akgul, M., Gumuskaya, E., Korkut, S. (2007). Crystalline structure of heat-treated Scots pine [*Pinus sylvestris* L.] and Uludag fir [*Abies nordmanniana* (Stev.) subsp. *bornmuelleriana* (Mattf.)] wood. *Wood Science and Technology*, 41(3), 281–289. DOI 10.1007/s00226-006-0110-9.
43. Gonzalez-Pena, M.M., Hale, M.D.C. (2009). Colour in thermally modified wood of beech, Norway spruce and Scots pine. Part 1: colour evolution and colour changes. *Holzforschung*, 63, 385–393.
44. Nuopponen, M., Vuorinen, T., Jamsa, S., Viitaniemi, P. (2003). The effects of a heat treatment on the behaviour of extractives in softwood studied by FTIR spectroscopic methods. *Wood Science and Technology*, 37(2), 109–115. DOI 10.1007/s00226-003-0178-4.
45. Song, J., Chen, C., Zhu, S., Zhu, M., Dai, J. et al. (2018). Processing bulk natural wood into a high-performance structural material. *Nature*, 554(7691), 224–228. DOI 10.1038/nature25476.